KAUNAS UNIVERSITY OF TECHNOLOGY
VYTAUTAS MAGNUS UNIVERSITY

GRAŽVYDAS KAZOKAITIS

RESEARCH AND DEVELOPMENT OF MAGNETOSPHERIC PIEZOELECTRIC DRIVE FOR ATTITUDE CONTROL OF NANO-SATELLITES

Summary of Doctoral Dissertation
Technological Sciences, Mechanical Engineering (T 009)

2021, Kaunas

This doctoral dissertation was prepared at Kaunas University of Technology, Institute of Mechatronics, during the period of 2016–2020.

Scientific Supervisor:
Prof. Dr. Vytautas JŪRĖNAS (Kaunas University of Technology, Technological Sciences, Mechanical Engineering, T 009).

Editor: Brigita Brasienė (Publishing house "Technologija")

The official defence of the dissertation will be held at 10 a.m. on 21th of May, 2021 at the public meeting of the Dissertation Defence Board of Mechanical Engineering Science Field in Dissertation Defence Hall at Kaunas University of Technology.

Address: K. Donelaičio Str. 73-403, 44249 Kaunas, Lithuania.
Tel. no. (+370) 37 300 042; fax. (+370) 37 324 144; e-mail: doktorantura@ktu.lt.

The summary of dissertation was sent on 21 of April, 2021.
The doctoral dissertation is available on the internet http://ktu.edu and at the libraries of Kaunas University of Technology (K. Donelaičio Str. 20, 44239 Kaunas, Lithuania), and Vytautas Magnus University Agriculture Academy (Studentų St. 11, Akademija, 53361 Kauno raj., Lithuania).

KAUNO TECHNOLOGIJOS UNIVERSITETAS
VYTAUTO DIDŽIOJO UNIVERSITETAS

GRAŽVYDAS KAZOKAITIS

MAGNETOSFERINĖS PJEZOELEKTRINĖS PAVAROS, SKIRTOS NANOPALYDOVAMS ORIENTUOTI, KŪRIMAS BEI TYRIMAI

Daktaro disertacijos santrauka
Technologijos mokslai, mechanikos inžinerija (T 009)

2021, Kaunas

Disertacija rengta 2016-2020 metais Kauno technologijos universiteto Mechanikos inžinerijos ir dizaino fakulteto Mechatronikos institute.

Mokslinis vadovas:
Prof. Dr. Vytautas JŪRĖNAS (Kauno technologijos universitetas, technologijos mokslai, mechanikos inžinerija, T 009).

Redagavo: Brigita Brasienė (Leidykla „Technologija")

Mechanikos inžinerijos mokslo krypties disertacijos gynimo taryba:
Dr. Rolanas DAUKŠEVIČIUS (Kauno technologijos universitetas, technologijos mokslai, mechanikos inžinerija, T 009) – **pirmininkas**;
Habil. Dr. Algimantas BUBULIS (Kauno technologijos universitetas, technologijos mokslai, mechanikos inžinerija, T 009T 009);
Prof. Dr. Sergėjus BORODINAS (Vilniaus Gedimino technikos universitetas, technologijos mokslai, mechanikos inžinerija, T 009);
Habil. Dr. Evgeniya KOROBKO (A. V. Luikov šilumos perdavimo ir masės kaitos tyrimų institutas, Baltarusijos mokslų akademija, technologijos mokslai, medžiagų inžinerija, T 008).

Disertacija bus ginama viešame mechanikos inžinerijos mokslo krypties disertacijos gynimo tarybos posėdyje 2021 gegužės 21 d. 10:00 val. Kauno technologijos universiteto disertacijų gynimo salėje.

Adresas: K. Donelaičio g. 73-403, 44249 Kaunas, Lietuva.
Tel. (+370) 37 300 042; faks. (+370) 37 324 144; el. paštas: doktorantura@ktu.lt.

Disertacijos santrauka išsiųsta 2021 balandžio 21 d.
Su disertacija galima susipažinti internetinėje svetainėje http://ktu.edu ir Kauno technologijos universiteto bibliotekoje (K. Donelaičio g. 20, 44239 Kaunas) ir Vytauto didžiojo universiteto žemės ūkio akademijos bibliotekoje (Studentų g. 11, Akademija, 53361 Kauno raj.).

INTRODUCTION

Relevance of the research

Nowadays, various modern systems, devices with precision drives use piezoelectric materials. The properties of piezoelectric materials are well known and used in a variety of industrial, scientific, and commercial products. The devices with piezoelectric drive can be installed in optical and laser systems, micromanipulators and robots, metrological devices, medical devices, precision material processing machines [1, 2]. Piezoelectric drives are precise, compact, and lightweight; they have low inertia, and the response time is fast. All these properties allow to achieve a high power-to-mass ratio in situations where such requirements exist and piezoelectric devices are used.

Piezoelectric drives are made from non-magnetic materials with ferroelectric properties that can be used where magnetic field or interference with it is undesirable [3]. These drives are silent; thus, they can be used in such cases where ambient noise is undesirable, for example, drug delivery systems, smart wearable devices, precise measurement devices [4, 5]. The control of piezoelectric devices is quite simple: when the device is excited by an electric control signal, the piezoelectric drive can perform linear or angular displacement. The power consumptions of piezoelectric devices are low; these devices are extremely efficient when the output power of drive does not exceed several dozen W, compared to the traditional electromagnetic drives. Piezoelectric drives do not require lubrication; thus, such drives are suitable for use where lubrication is not desirable or impossible to realize, the evaporation of oil is restricted, for example, in vacuum [6, 7]. Low self-heating of the piezoelectric drives while they are in operation mode allows to use such drives where the heat generation is unacceptable. Piezoelectric drives are capable to operate at extremely low temperatures, up to several kelvins [8]. The design is relatively simple, i.e., several moving parts and unsophisticated control; the cost of such drives or devices are relatively low. Piezoelectric drives are easily adapted to the requirements and suitable for various tasks where the advantages of the piezoelectric materials and drives can be availed.

Piezoelectric drives have been studied in detail as a possible replacement for typical electromechanical drives, but despite the advantages, which were mentioned above, these types of drives as well have certain disadvantages that limit the possible usability of such drives: the displacement value, which is achieved from the drive, and the size of the drive cannot be enlarged. Sometimes, the insufficient accuracy of gears, the wear of contact surfaces, the production cost of the drive or device become economically unprofitable. Thus, a number of studies and analysis are still underway to modify and improve this type of drives

and actuators to avoid or reduce the aforementioned shortcomings and related issues [6, 9, 10].

In order to use piezoelectric drives in satellites, it should be noted that this type of drives requires a control module and power source to ensure stable operation of the actuator as well as measuring and feedback systems, but these drives are small and lightweight and can be integrated in small volume and do not increase the mass of the satellite significantly. Piezoelectric drives consume small amounts of energy; the positioning accuracy is very high; they do not require lubrication and can operate at low temperatures and high vacuum.

Aim of the research

The aim of this study is to develop and investigate multi-degree of freedom magnetospheric piezoelectric drive (MPD) for the active attitude control of nanosatellites. In order to achieve this aim, the following objectives have been set:

1. To perform the analysis of existing piezoelectric drives in order to determinate the possibilities of their usage for active and passive attitude control of nanosatellites, to improve satellite positioning accuracy and energy efficiency characteristics;
2. To design numerical models of piezoelectric drive for the active 3D attitude control of nanosatellites in space and perform analysis of its control modes and perform the analysis of dynamic characteristics and influence of transducer's control electrode configuration on multidirectional vibration excitation;
3. To create an experimental setup of a drive with the piezoelectric actuators, taking into account analytical calculations and perform experimental studies of control modes and dynamic characteristics with this setup;
4. Using the developed piezoelectric drive with a magnetic spherical rotor, to perform the simulation of a nanosatellite, orbiting a given trajectory around the Earth, for its 3D orientation in space and present the conclusions.

Methods of the research

This research work is prepared using theoretical and experimental research methods. The following software packages and equipment were used to create and analyze 3D models: Autodesk Inventor Professional 2018, COMSOL MultiPhysics 5.3, Microsoft Excel and Matlab 2017a with plug-ins Simulink, and Smart Nanosatellite Attitude Propagator (SNAP) V3.0.

The experimental studies were performed in the laboratories of Kaunas University of Technology, Institute of Mechatronics. Laser Doppler vibrometers (LDV) Polytec PSV 500-3D-HV and OFV-5000/505 and a signal generator WW5064 (Tabor Electronics Ltd.), a voltage amplifier EPA-104 (PiezoSystems

Inc.) were used to investigate the dynamic characteristics of vibrations of piezoelectric drive and displacement measurements. Wayne Kerr 6500B impedance analyzer was used for impedance research. A three-axis magnetometer, Model 460 (Lake Shore Cryotronics, Inc.), was used for measuring the strength of the spherical rotor's magnetic field.

Scientific novelty

1. A novel magnetospheric piezoelectric drive has been developed. This drive rotates the sphere in 3D trajectories and has a high positioning accuracy of the spherical rotor, which allows to perform 3D attitude control of the satellite in space;
2. Piezoelectric ultrasonic actuator, which operates in higher oscillation modes, has been designed, developed, and researched; the geometrical parameters of the transducer of the drive have been determined and calculated for the higher mode oscillations, and the electrode configuration, which is required for efficient control, was analyzed;
3. Numerical models of unimorph ring-type piezoelectric actuator for the motion trajectories were developed and investigated.

Defended statements

1. An ultrasonic piezoelectric drive with a spherical rotor was developed. This drive has high angular displacement accuracy (resolution 30 ±rad ± 1 μrad) and can be used in small satellites for active 3d attitude control systems in Space.
2. An ultrasonic piezoelectric actuator, which operates in resonant frequency ~ 95 kHz, has been developed and investigated. Geometrical parameters and dynamic characteristics of the actuator, which are crucial to find the most efficient configuration of its control electrode segmentation, have been determined, calculated, and analyzed.
3. Numerical models of unimorph type piezoelectric ring-shaped actuators have been developed to analyze the amplitudes and trajectories of spatial oscillations and resonant operating frequencies of its contact points.

Practical value

1. 3D numerical models of piezoelectric drive have been developed; these models can be used to perform calculations, analyze various drive configurations, perform theoretical research;
2. A multichannel electrical signal control module that can be used to investigate piezoelectric ultrasonic drives with different control electrode configurations and/or different geometry piezoelectric transducers was developed;

3. The developed and researched unimorph ring-type piezoelectric actuator with improved flange geometries and multimode oscillations ensure higher accuracy of spherical rotor angular motion, and it is more energy efficient;
4. The developed piezoelectric drive design can be used for active attitude control of the satellite as well as in robotics, optomechanical engineering and in other cases where precision positioning is necessary.

The obtained research results were applied to the R&D project "High resolution multi-DOF piezoelectric systems for precision technologies" (No. 01.2.2-LMT-K-718-01-0010), funded by the EU under Measure 01-2.2-LMT-K-718 "Targeted Research in Smart Specialization Areas".

Research approbation

The results of the research were published in 2 journals with impact factor indexed in Web of Science database and 4 conference proceedings.

The results were as well presented in 6 scientific conferences (Mechanika 2017, Mechanika 2019 (Kaunas, Lithuania); Vibroengineering 2017 (Vilnius, Lithuania); Conference on Advance Robotics, Mechatronics and Artificial Intelligence 2018 (Valencia, Spain); Conference on Smart Materials and Structures 2019 (Dublin, Ireland); Mechatronic Systems and Materials 2020 (Bialystok, Poland)).

Moreover, the design of the magnetospheric piezoelectric drive was patented, Patent no. LT 6728 B, 2020-04-10.

Structure of the dissertation

The dissertation consists of an introduction, four chapters, general conclusions, a list of references and scientific publications on the topic of the dissertation, and appendixes.

The volume of the dissertation is 132 pages, 40 formulas, 110 figures, and 19 tables. The list of references consists of 117 sources.

1. LITERATURE REVIEW

Small satellites can be classified according to various properties: weight, orbit, purpose, etc. Usually, small satellites are classified by mass property. The mass of small satellites can vary from 100 kg to 1 g. The most popular class is nanosatellites. The weight of these satellites is 1–10 kg.

The most popular group of small satellites is CubeSat. This group belongs to the class/category of small satellites that are used by universities, commercial entities, or even amateurs and their groups. CubeSat satellites have strict rules and requirements, related to the design and the arrangement of the internal components of the nanosatellite [11, 12, 13]. According to these requirements, nanosatellite has a minimum dimension of 10×10×10 cm and the mass of 1.33 kg. Such a single

volumetric and mass unit is relatively denoted as 1U. In practice, larger-sized satellites have iterative sizes: 1.5U, 2U, 3U, 6U, etc. Such definition means that the satellites do not change the length and width dimensions, but the height of the satellite changes.

When a satellite is in the orbit during a mission, the positioning and orientation mechanism is needed to define and determinate the position of the satellite in space and adjust it if necessary. For the attitude control of the satellite, several different techniques can be used: passive, semi-active, and active systems [14]. Passive systems commonly use permanent magnets, gravitational gradient mechanisms. When the permanent magnet is used, they orientate satellite together with the Earth's magnetic field. In semi-active systems, various electromagnetic mechanisms and devices are used. Some satellite designs have actively moving mass, which can be moved and change the center of gravity of the satellite. Active systems are complicated and use liquid propellants, fast moving masses (gyroscopes), plasma engines. Such systems require high energy consumption to operate. The mentioned systems have certain advantages and disadvantages: if the system is passive, it does not use energy, but does not allow to control the satellite after it has launched. If the system is active, it is complicated, consumes a lot of energy. Therefore, an innovative solution that proposes a system that is small in size and mass with extremely low energy consumption and ability to control the attitude is always relevant.

One of the possible technological solutions can be drives with piezoelectric elements. Piezoelectric devices are able to meet the most of the requirements: fast, uncomplicated, relatively cheap, do not interfere with the magnetic fields, do not require lubrication, and the consumption of energy is extremely low. Piezoelectric drives are widespread in a variety of disciplines where high accuracy and reliability is required; thus, such drives are very popular in various devices in such areas as aerospace, military, aviation, metrology, precision equipment industry, and others.

2. NUMERICAL STUDIES

2.1. Design concept of magnetospheric piezoelectric drive and operating principle

The proposed MPD consists of two ring-type piezoelectric transducers, two flanges, which are bonded (glued) with the transducers, and aspherical permanent magnet rotor. Such assembly creates 3D rotary motion drive with two piezoelectric unimorph-type actuators. These flanges are used for integration and are combined with the satellite's chassis. The flanges are connected using studs and bolts. Such design allows to pre-load the system equally for each contact element and fix the rotor. Spherical rotor is placed between two piezoelectric transducers, and the

rotor rests on 6 contact elements. These contact elements (3 for each transducer) are glued on piezoelectric transducer. The schematic view of the drive is shown in Figure 2.1.

When an electrical signal excites the piezoelectric transducers, the magnetic sphere is rotated. Two ring-type piezoelectric transducers are placed opposite to each other in order to apply the pre-load to the rotor as evenly as possible and increase its torque. This design principle can be widely used for various applications, not only for satellites, but as well in robotics, laser beam control systems, etc., where precise and energy-efficient 3D rotary positioning system may be desirable.

The structure of the proposed MPD: a spherical rotor (*2*) is inserted between two ring-type piezoelectric transducers (*3*) and rests on three friction-resistant contact elements (*4*), which are glued on the transducers (*3*). Two electrodes of the piezoelectric transducer are located on the flat surfaces. On one side, the ground electrode is not segmented; on the other side, the electrode is divided into three segments (green, red, and yellow), Figure 2.1 (b). In the centers of these electrodes, the contact elements are attached. The ground electrode of the transducer is monolithic, and the transducers are glued to a thin bronze flange (*1*). The MPD is symmetrical; thus, lower and upper sides are identical. These two halves are connected by using studs (*5*) and bolts (*6*).

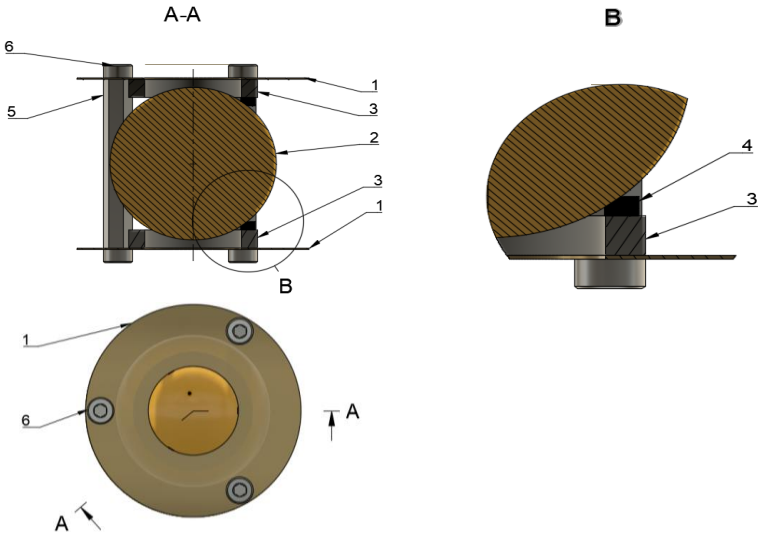

(a)

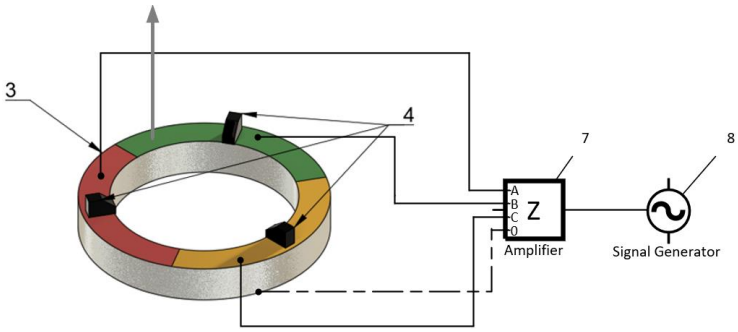

(b)

Figure 2.1. 3DOF MPD structure: 1 – flange, 2 – spherical permanent magnet rotor, 3 – piezoelectric transducer, 4 – contact element, 5 – stud, 6 screw, 7 – multichannel amplifier, 8 – electric signal generator, (a) schematic view, (b) a piezoelectric transducer with contact elements and a direction of polarization and electrical connection diagram

In Figure 2.1 (b), the electrical schematic view of proposed MPD is shown. The electrical signal generator (*8*) is connected to a multichannel amplifier (*7*). This amplifier has three channels: A, B, and C, and one common ground channel O to which non-segmented electrodes are connected. Each of the channels is electrically connected to a particular electrode of the piezoelectric transducer. The lower and upper transducers are electrically connected in parallel and connected to the corresponding channel of the amplifier. This connection method allows to excite two transducers simultaneously and amplify the generated mechanical force during excitation, which rotates the spherical rotor.

The working principle of this drive is based on the fact that when the piezoelectric transducer is excited by a harmonic electric signal of the defined frequency and amplitude, the transducer starts to oscillate in higher bending modes. The displacements are achieved when the piezoelectric transducer is excited at a higher harmonic resonant frequency. These displacements cause the transducer to deform in space, and the contact elements on individual points of the transducer begin to oscillate in an elliptical trajectory. These contact element oscillations with the impact on the surface of the spherical rotor, due to the acting friction, force the rotor to rotate in a desired direction. The rotational speed and output torque are controlled by the change of the excitation signal amplitude. Different segments of the piezoelectric transducer electrodes are excited to change the direction of rotation of the spherical rotor.

2.2. Numerical model of magnetospheric piezoelectric drive

The numerical MPD model (FEA model) is made by simplifying the CAD model. The FEA model consists of the essential components: a ring-type piezoelectric transducer, a flange, and contact elements. The drive is symmetrical; thus, there is no necessity to design the upper half of the drive. In the numerical studies of the drive, different simulation scenarios were considered, and the results of these simulation conditions are presented below.

The aim of numerical analysis was to find the resonant frequencies and geometrical parameters of the transducer and determine the amplitude-frequency characteristics, find out the frequencies, which are needed to ensure reliable 3D rotational motion of the rotor. During numerical analysis, two configurations have been considered, i.e., the dependence of oscillations' amplitude on different electrode segmentation configuration and on the shape of the flange. The simulations are performed in two stages: first, a numerical study of modal frequencies is performed, and later, based on the obtained results, the calculations of amplitude frequency characteristics are performed.

During numerical analysis, piezoelectric transducer was pre-loaded by 0.8 N force on contact elements, which mimics the weight of the spherical rotor. The transducer was constrained at three points at fixing holes. Piezoelectric and dielectric losses were neglected. However, the components have assigned mechanical damping coefficients of 0.001 and 0.004, respectively, for bronze and PZT-4 [15, 16].

Comsol Multiphysics was used for numerical analysis. FEA meshes for numerical models were created using tetrahedral elements that are proportionally applied (discretized) to each calculated element individually. The minimum mesh element size is 0.35 mm, the maximum 2.8 mm. The total number of nodes reaches ~ 145300 (transducer with disc flange) and ~ 110500 (transducer with triangle flange). The rational size of nodes was determined by iteration to achieve acceptable combination between calculation accuracy and duration. The views of the mesh of different design configurations are presented in Figure 2.2.

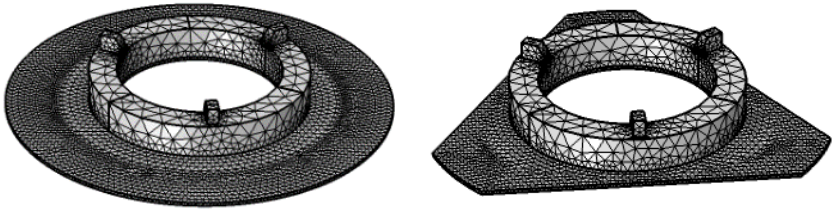

(a) (b)

Figure 2.2. Mesh views of different flange configurations of piezoelectric actuators: (a) actuator with disk-shaped flange, (b) actuator with triangle-shaped flange

2.3. Analysis of piezoelectric transducer with different electrode segmentation

The signal electrode was divided into three different configurations: 3 segments at every 120°, 6 segments at every 60°, and 9 segments at every 40°. Such segmentation was chosen because that minimum number of required contact elements for the positioning of spherical rotor is three contact elements. Separate 6 segments allow the area of electrode to be changed by dividing the signal electrode into 6 equal parts that the support elements would be arranged every 120°. Similarly, to the 9 segments, the latter divide the excitation electrode by evenly reducing the area and arranging the support contacts every 120°. The smaller area of electrode has a smaller electrical capacity; thus, it needs less energy for the excitation. Although this size does not differ much, the energy efficiency of the drive allows to use this type of drive in a system where energy costs are particularly relevant. Mechanically, if the drive is able to generate displacements of similar or higher amplitude with better electrical efficiency, the drive design is rationalized.

The piezoelectric transducer is lifted from the flange on three elastic supports; using this configuration, the flange is almost independent from the piezoelectric transducer. The contact supports separating the flange from the transducer are placed at the points where the signal electrode is divided equally from the contact supports. Numerical models with different electrode configurations are presented in Figure 2.3.

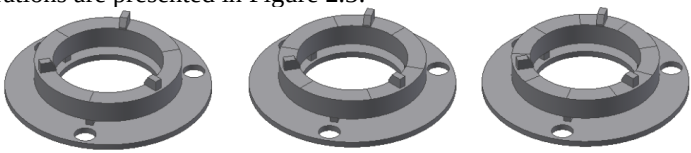

(a) (b) (c)

Figure 2.3. Numerical models of ring-type transducers with flange and different excitation electrode segmentations: (a) 3 segments, every 120°, (b) 6 segments, every 60°, (c) 9 segments, every 30°

Numerical analyzes have been done in the wide frequency range (50–110 kHz); several operating modes have been determined when the displacements dominate in the axial (Z) and radial (X) directions. Their displacements in these directions are necessary for the rotation of the sphere. Analyzing the obtained results, it has been found that sphere rotation is possible at a modal frequency of 91.15 kHz.

The harmonic response analyzes had been performed when the piezoelectric transducer was excited by a 100 V electrical signal, exciting only one piezo-segment. This has been done because a) the system is symmetric, b) in a real

system, only one piezo-segment is excited at a certain time. Harmonic response studies were based on the results of numerical studies of modal frequencies and forms. For further studies, the frequency range from 85 kHz to 110 kHz was chosen. In harmonic response studies, three possible cases are considered: the signal electrode is divided into three, six, and nine equal segments. The influence of electrode segmentation on displacements and oscillation amplitudes on the X, Y, and Z axes is shown in Figure 2.4. It should be noted that Z axis is aligned with the rotational axis of the transducer; the X axis is aligned with the center of the electrically excited piezo-segment and passes through the center of the contact element; X coincides with the radial axis of the actuator.

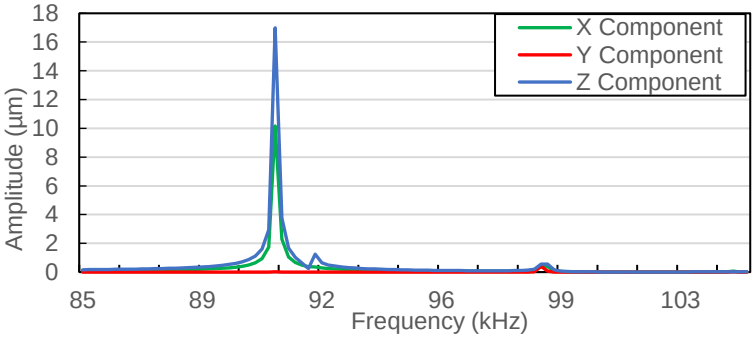

(a)

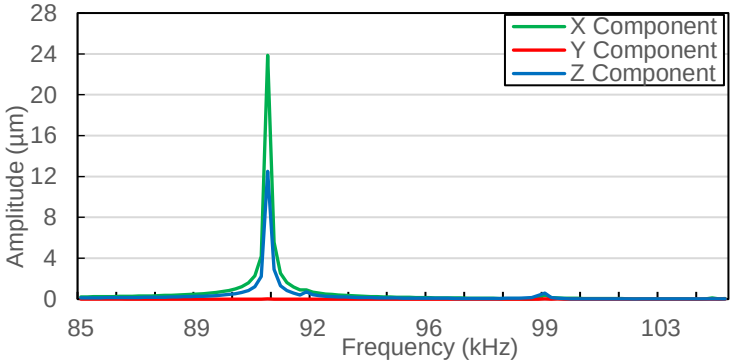

(b)

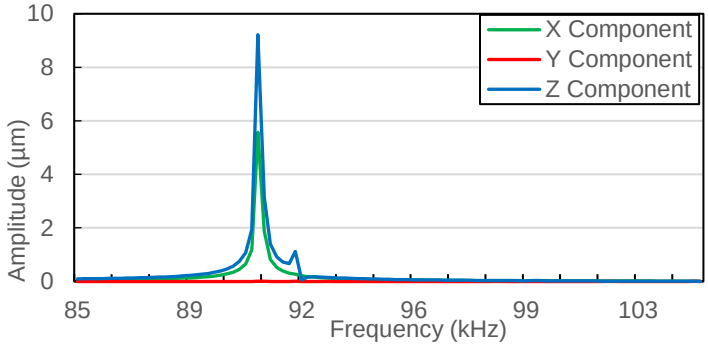

(c)

Figure 2.4. Results of harmonic response analysis when the signal electrode is divided into: (a) 3 segments, (b) 6 segments, (c) 9 segments (vibration modes at 90.80 *kHz*)

The graphs show that the vibration amplitudes are dominating in X and Z directions, and the number of segmented electrodes influences the amplitudes of vibration. The highest oscillation amplitude in X direction is equal to 23.9 µm and is achieved when the top electrode is divided into 6 segments. It is 2.4 times larger value compared to the amplitude obtained when the electrode has three segments. The highest amplitude in Z direction that is equal to 17.1 µm is obtained when the electrode is divided into three segments, and it is 25% bigger compared to the amplitude when the electrode is divided into six sections. Moreover, it must be noticed that the vibration amplitude in the Y direction is close to zero at the frequency of 90.80 kHz, but the amplitude peak can be seen at the frequency of 99.21 kHz, Figure 2.4 (b). The amplitude value at this peak is 0.41 µm, and it is much smaller compared to the amplitudes of vibration in X and Z directions shown in Figures 2.4 (a), (b) at the frequency of 90.80 kHz.

2.4. Numerical studies of piezoelectric transducer with different flanges

In order to design and develop a more rational MPD design, reducing the size, weight, and at the same time energy consumption of the drive itself, the actuator design has been modified to the unimorph-type unit with the flange. In this case, the piezoelectric transducer was glued to a thin bronze flange. This resilient bronze flange can be used as a fastening element in the system. The flange must be symmetrical with a small number of angles, because otherwise, if the number of angles increased, the energy losses would occur and the amplitudes of the displacements would decrease. Therefore, two possible designs will be considered: when the flange has no angle (disc shaped) and has three angles with

three mounting holes. The geometry and sizes of the actuators are shown in Figure 2.5.

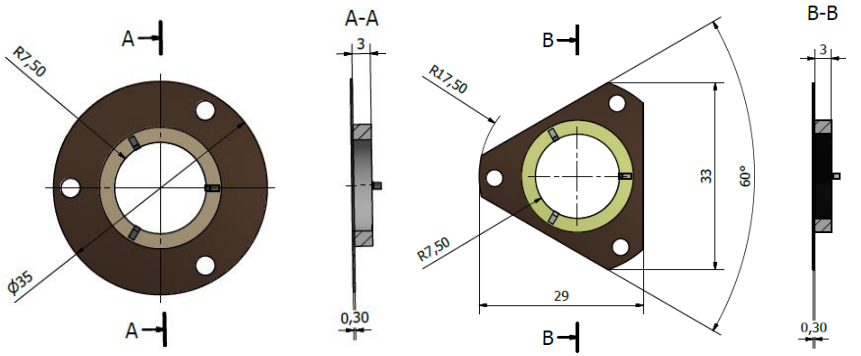

(a) (b)

Figure 2.5. Dimensions of actuators and flanges: (a) actuator with disc-shaped flange, (b) actuator with triangle-shaped flange

The oscillation frequency range from 50 kHz to 110 kHz was chosen for modal frequency and shape analysis. In these studies, it was found that the modal frequencies of the piezoelectric actuator in the radial and axial directions can be achieved at several resonant frequencies. One such frequency is 93.2 kHz. The needed modal shapes were determined at the frequencies of 94.8 kHz and 95.3 kHz for the actuators with a disc and triangle-shaped flanges.

Harmonic response analysis of the actuator has been performed. The aim of numerical simulations was to determinate the rebound of the contact element and find out its trajectory of motion while voltage is applied to one of the segmented electrodes. The amplitude of the driven electric signal was 50 V, and this signal was provided for one of the signal electrodes, while the bottom electrode was grounded. The analysis was performed in a frequency range of 85–105 kHz, while the solution step was 50 Hz. The piezoelectric actuator has a symmetrical structure. Hence, only one segment of the top electrode was excited. Numerical simulation was performed when the actuator had a disc-shaped and triangle-shaped flange, respectively. The displacement amplitudes in X, Y, and Z directions were studied and compared. The results of the harmonic response analysis are presented in Figure 2.6.

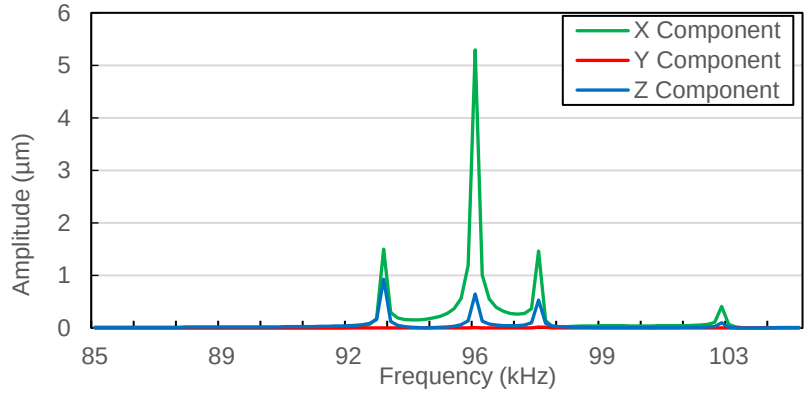

(a)

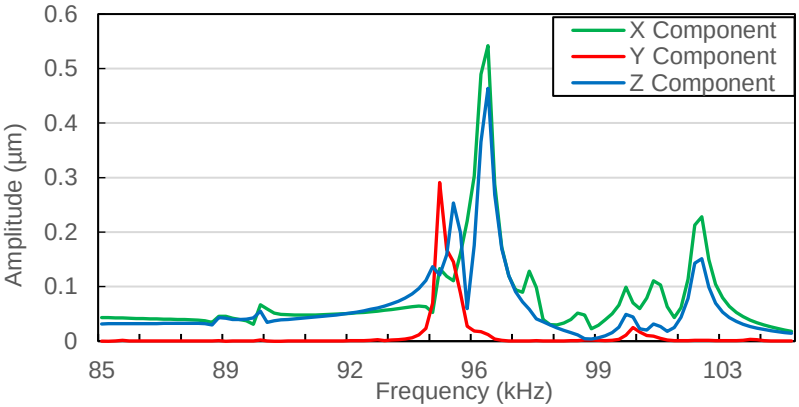

(b)

Figure 2.6. Results of numerical analysis of harmonic response: (a) disc-shaped flange, resonance mode 95.8 *kHz*, (b) with the triangle-shaped flange, resonance mode 96.2 *kHz*

From the graphs, it can be seen that the dominant vibrations appear in radial and axial directions, i.e., X and Z accordingly, and the shape of the flange has a big influence on the displacement amplitude. The higher amplitude was determined in the X-axis direction for the actuator with a disc-shaped flange. The value of this displacement is 6.2 µm. The axial displacements in the Z-axis direction are as well for the actuator with a disc-shaped flange and equal to 0.92 µm. It must be noted that using a triangle shape for the flange, the vibration amplitude is significantly smaller compared with the disc-shaped actuator. The actuator with a disc-shaped flange reaches its resonant peak at 95.8 kHz, while the

actuator with a triangle-shaped flange at a frequency of 96.2 kHz. The amplitudes in X and Z directions decrease accordingly with the higher resonant frequencies. In conclusion, disc-shaped flange is more suitable for the usage, because the actuator with such flange can reach higher amplitudes.

3. EXPERIMENTAL STUDIES

3.1. Experimental setup

In order to perform experimental studies and validate numerical analyzes, several experimental setups have been made. These prototypes were designed and made according to the numerical models. All materials and geometry correspond to the numerical models, which were used for numerical studies. In Figure 3.1, the experimental setups are shown.

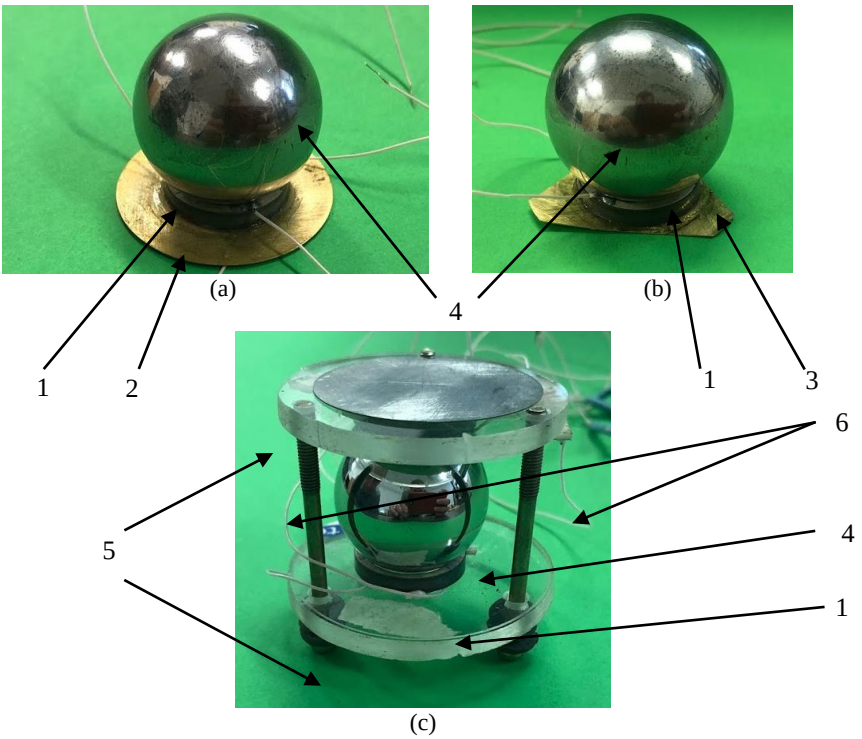

Figure 3.1. Piezoelectric actuators and drive: a) actuator with disc shaped flange, b) actuator with triangle shaped flange, c) assembled drive, 1 – piezoelectric transducer, 2 – disc shaped flange, 3 – triangle shaped flange, 4 – spherical rotor, 5 – enclosing disks, 6 – stud

3.2. Measurement of electrical impedance of piezoelectric actuator

For the evaluation and verification, the results of numerical studies related to the calculated resonant frequencies and modal shapes of piezoelectric actuator, impedance analysis of piezoelectric transducers have been performed. An impedance meter Wayne Kerr 6500B was used. The following cases were investigated:

- Assembled drive;
- Piezoelectric transducer with differently segmented electrodes;
- Actuator with disc type flange;
- Actuator with triangle shaped flange.

Piezoelectric transducers were segmented using the same pattern like it was in the numerical studies: three, six, and nine equal segments. The results of impedance measurement of differently segmented piezoelectric transducers show that increasing the number of segments, the impedance (Z (Q)) values increase as well, when the piezoelectric transducer is in resonant mode. This value increases from ~ 260 kΩ (3 segments), ~ 390 kΩ (6 segments), to ~ 580 kΩ (9 segments). The change of the phase angle (θz) changes with increasing number of segments: from 52° (3 segments), 32° (6 segments), to 27° (9 segments). When the transducer is in the operating resonant mode, the operating frequency of the oscillations varies from 92 kHz to 95 kHz.

It can be noted that the resonance quality of a transducer with 6 piezo-segments differs slightly from the case when the electrode is divided into 3 segments. It can be concluded that it is most effective and can and should be used for further development, because the electric capacity of such a converter is smaller and such a drive is more energy efficient. The results of impedance measurement while the transducer is divided into 6 segments are shown in Figure 3.2.

Further measurements were performed by measuring actuator with flanges with different shapes. From the measurement results, it has been observed that the impedance quality of the actuator with a triangular flange is lower than that of the actuator with a disc shaped flange. The results of the following measurements have been obtained, i.e., the impedance (Z (Q)) values when the piezoelectric transducer is in resonant mode: ~ 190 kΩ (actuator with disc flange), ~ 104 kΩ (actuator with triangular flange); the variation of the phase angle (θz) depending on the flange geometry: 18° (actuator with disc flange), 28° (actuator with triangular flange). When the actuators are in resonant mode, the operating resonant frequency is ~ 96 kHz (disc flange) and ~ 94 kHz (triangular flange). The measurement results of actuator with the disc flange are presented in Figure 3.3.

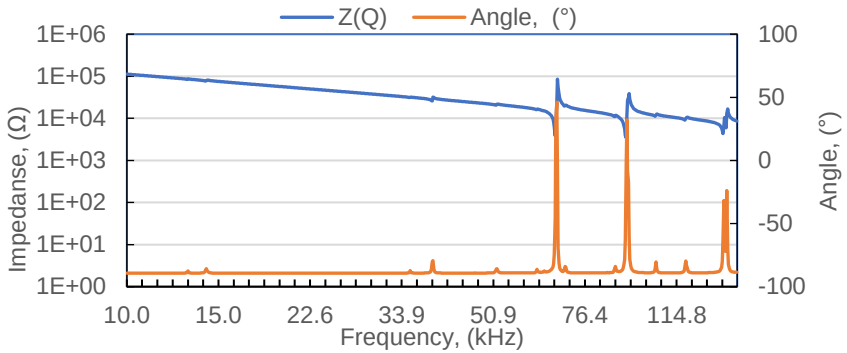

Figure 3.2. Results of transducer impedance measurements when the excitation electrode is divided into 6 piezo-segments

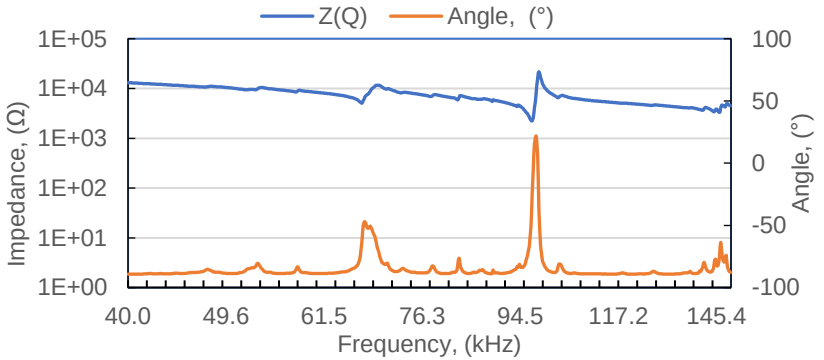

Figure 3.3. Results of the impedance measurements when actuator has disc shaped flange

3.3. Experimental studies of modal frequencies and shapes

In order to evaluate whether the determined values of the operating resonant frequencies of the drive are acceptable and expand the understanding of the basic dynamic characteristics related to the piezoelectric actuator, it is necessary to perform validation of the modal frequencies and shapes and harmonic response characteristics, which were calculated in numerical studies. 3D laser scanning techniques based on laser Doppler vibrometry (LDV) were used in these studies.

These studies use a 3D scanning LDV system Polytec PSV-500-3D-HV with PSV 9.2 software. The transducer was glued to the massive steel plate using a resilient double-sided adhesive tape. The measurements of a piezoelectric actuator glued with a disc shaped flange and a piezoelectric transducer glued with

a triangle shaped flange were performed. The resonant frequencies of the elements were considered in the range of 50 kHz to 110 kHz.

Figure 3.4 shows the scan results when the piezoelectric transducer is "softly" (with an elastic double-sided adhesive film) glued to a steel plate. The measurements showed that the piezoelectric transducer has two clearly expressed resonant frequencies, i.e., at 61 kHz and at 92.8 kHz. Figure 3.5 shows the measurement results when the piezoelectric actuator is bonded to the disc flange. In this case, the resonant frequencies of the actuator were reached at 64.8 kHz and 93.72 kHz. Figure 3.6 shows the measurement results when the piezoelectric actuator is bonded to the triangle shaped flange. The resonant frequencies of the actuator were reached at 65.8 kHz and 94.4 kHz.

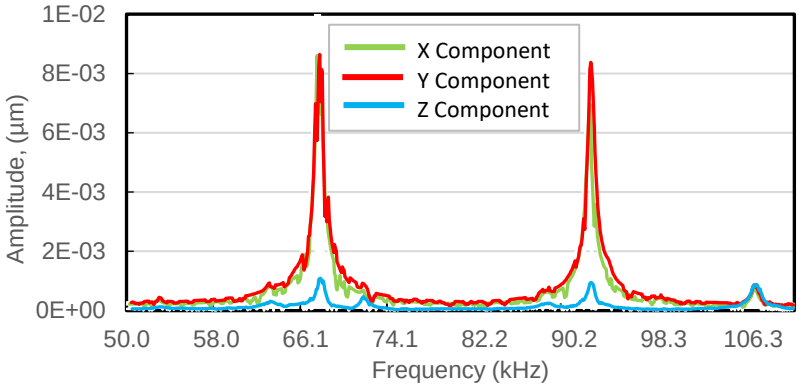

Figure 3.4. Measured amplitude and frequency dependence of piezoelectric transducer elastically fixed to a steel plate under resonant frequencies at 61 kHz and 92.48 kHz

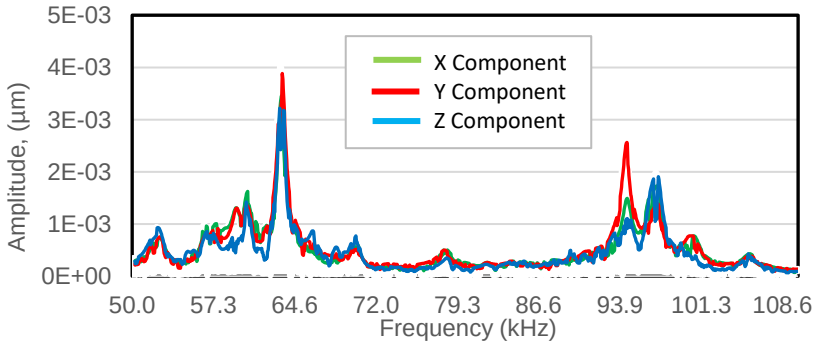

Figure 3.5. Measured amplitude and frequency dependence of piezoelectric actuator fixed to disc shaped flange under resonant frequencies at 65.8 kHz and 94.4 kHz

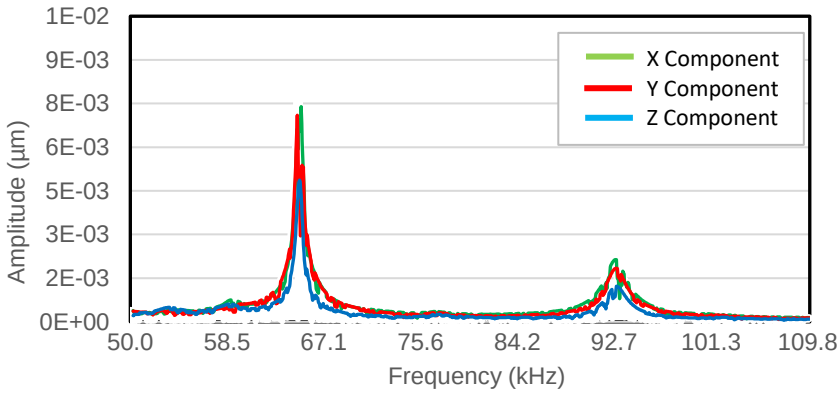

Figure 3.6. Measured amplitude and frequency dependence of piezoelectric actuator fixed to the triangle shaped flange under resonant frequencies at 64.8 kHz and 93.72 kHz

According to the impedance measurement results described above, the operating resonance frequency range is between 90 kHz and 95 kHz. This frequency range was chosen because, despite the fact that at ~ 60–65 kHz excitation, the displacement amplitudes are higher, but the operation of the drive itself is less predictable, and it is harder to control rotation direction; the movement of the sphere is with some steps; the speed of the rotation is inconsistent; thus, the operating frequency range of 90–95 kHz was chosen accordingly. It is as well worth mentioning that the determined operating frequencies are very similar to those selected in the FEA models. The difference between numerical and natural experiments is 1% with a triangular flange and 3% with a disc-shaped flange, respectively.

In summary, it can be stated that the determined resonant frequencies in piezoelectric actuators cause such oscillations that allow to rotate the spherical rotor smoothly; the direction of rotation depends on the excited electrode segment of the transducer or their pairs. This confirms that the operating frequencies have been set correctly.

3.4. Resolution measurements of magnetospheric piezoelectric drive

The study was performed by the excitation of a piezoelectric actuator by a harmonic high-frequency burst-type signal obtained from a signal generator. The experimental setup was placed on a rubber base. The spherical rotor was placed on the contact supports without the use of any additional force, except for the gravitational force of the rotor itself.

During the measurement of the displacement resolution, the drive operated in step mode, during which, the angular displacement of the one-step rotor was generated. One of the piezo-segments with the following electrical signal parameters was excited:

- Excitation signal type is burst-type;
- Number of bursts per second is 1;
- Amplitude of the signal is 60 V;
- Signal frequency is 92 kHz.

It was experimentally determined that when the actuator is excited in steps, every 1 sec with harmonic burst-type signal, containing 20 periods of the signal of 92 kHz frequency and voltage amplitude of 60 V, the average resolution (value of one step) of rotation angle that is equal to 30± 1 μrad is obtained. The measurement results are shown in Figure 3.7.

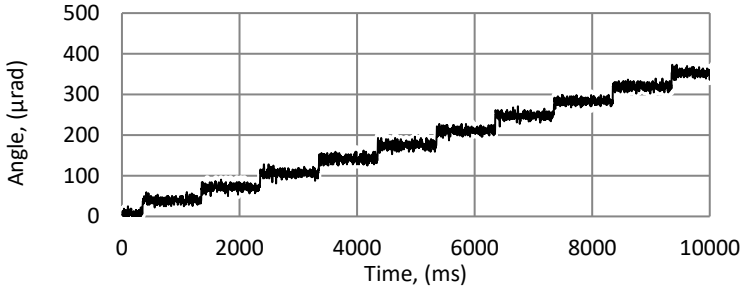

Figure 3.7. The results of the measured resolution by performing angular displacement of the spherical rotor

3.5. Displacement measurements of the active point of the transducer

The experiments were performed to verify the spatial oscillations of one active contact point located on the excited piezoelectric transducer. During these measurements, a piezoelectric transducer is excited by an operating harmonic electrical signal, and the amplitude of the active point oscillations in the radial and axial directions is measured with a 3D scanning laser vibrometer.

During the experiment, the operating resonant frequency was set to 95.1 kHz and the signal amplitude to 50 V for the excitation of the actuator with a disc-shaped flange. The operating resonant frequency when measuring the actuator with a triangle shaped flange is 94.6 kHz, and the voltage is 50 V. The results are presented in Figure 3.8 (a), (b).

From the results, it can be seen that the contact point motion trajectories have ellipsoidal shapes. However, this trajectory is not ideal. This was due to the

measurement errors, environmental vibrations, and manufacturing and assembling errors of the piezoelectric actuator.

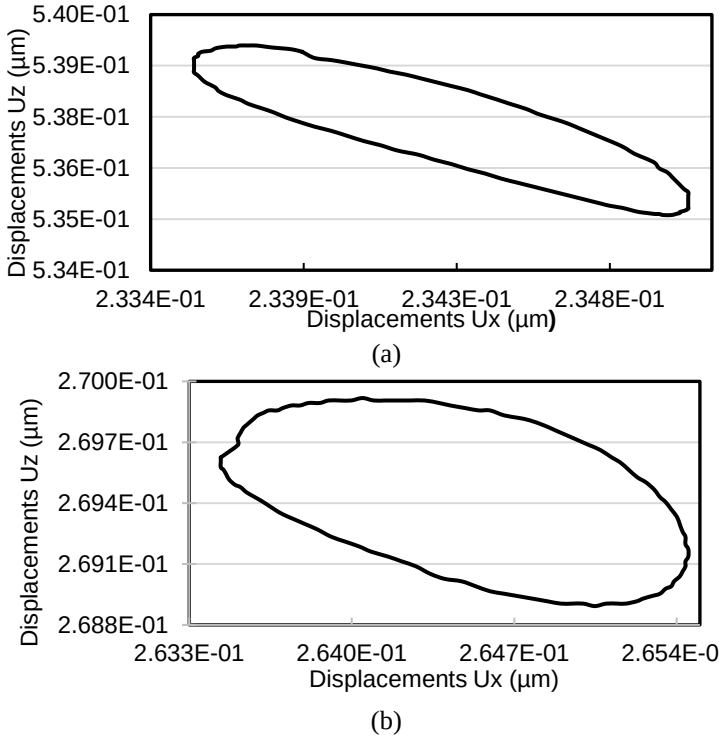

Figure 3.8. Contact point oscillation trajectories: (a) actuator with a disc shaped flange at a resonant frequency of 95.1 kHz, b) actuator with triangle shaped flange at a resonant frequency of 94.6 kHz

3.6. Measurements of the rotation frequency of the spherical rotor

In order to find out the maximum angular velocity of the spherical rotor at the steady-state operation mode of the drive, the experiments were performed, in which the average values of angular speed were determined by using actuators with differently shaped flanges. The number of revolutions of the sphere was measured for a certain time.

After several tests, the mean values were found: when the actuator with a disc shaped flange was used, at a resonant frequency of 94.4 kHz and an excitation voltage of 70 V, the spherical rotor speed reached 30 rpm ±2rpm. Meanwhile, if

an actuator with a triangle shaped flange and excitation of 93.8 kHz and 70 V was used, the rotation speed was 27 rpm ±2rpm.

4. NUMERICAL STUDIES OF SATELLITE MISSION

4.1. Tools for numerical simulation of satellite mission

In order to perform the analysis of the attitude control system of the nanosatellite equipped with a MPD described in this work, numerical simulations are performed using the SNAP (Smart Nanosatellite Attitude Propagator) tool and act as an add-on to Matlab in a computing environment [17, 18, 19].

This Matlab add-in is designed to perform simulations and allow to analyze various parameters encountered during the mission planning and testing. Because launching a satellite into a mission to test the proposed drive or designing and producing the whole satellite is financially unprofitable and inefficient, numerical simulations are used. SNAP tool is capable of performing calculations based on the set parameters of the mission and satellite systems. Such testing is common, and a number of tools have been developed that are used to perform such simulations [17, 20, 21]. SNAP was developed as a tool to perform simulations on KySAT-1 and KySAT-2 satellites (is a CubeSats of 1U size) that were launched into the orbit in 2011–2013 and have successfully completed their missions. This tool was later improved and made for the public use.

4.2. Integration of magnetospheric piezoelectric drive into the satellite's chassis

Numerical simulations will be based on 1U ESTCube-1 satellite. This satellite has well described detailed structure, mission parameters, and telemetry. In this way, the selected prototype had a practical assessment in the already existing system.

In order to perform simulations and analysis of attitude control of the ESTUCube-1 satellite using developed MPD, some modifications in the satellite structure were studied. Instead of the attitude control system components used in ESTUCube-1 (dissipated mass, electromagnetic coil, mechanical drive, and control system), the new components of MPD will be inserted for the attitude control of the satellite.

Trying to keep the system as minimally modified as possible, the previous satellite design was changed that the former attitude control mechanism would be replaced by the MPD. The implementation of this change is shown in Figure 4.1. The structure of the satellite is simplified. The mass values, which were changed due the modifications of the attitude control system, are shown in Table 4.1.

Table 4.1. The changes in mass using modified attitude control mechanism

System	Mass (g)	
	ESTCube-1	ESTCube-1 mod.
Chassis	287	
Electrical power system	291	
Command and data handling	49	
Communication	75	
Tethering mass	206	-
Tethering and photographing	30	
Attitude determination and control	112	**160**
Total	1050	**892**

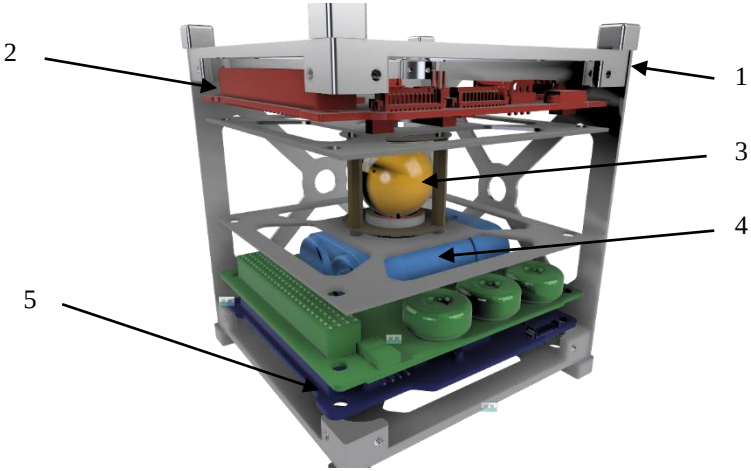

Figure 4.1. The structure of modified design of ESTCube-1 satellite: 1– satellite chassis, 2 – attitude determination and control system (ACDS), 3 – MPD, 4 – electrical power system, 5 – communication system

Using ESTCube-1 telemetry and flight data, the simulations are performed that will derive results on the behavior of the modified satellite during the mission. In Figure 4.2, the necessary data are entered which were obtained using accessible sources [22, 23, 24, 25, 26, 27, 28].

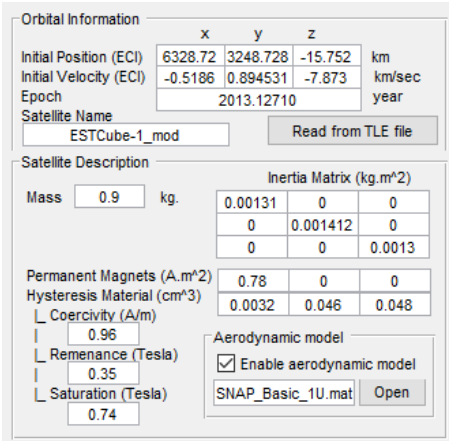

Figure 4.2. The main values which are needed for the simulations

The satellite in orbit is constantly exposed to certain forces: atmospheric, gravitational gradient, solar pressure, and magnetic. These forces can operate in different ways: continuously, depending on the height of the orbit, depending on the conditions, etc. A summary graph showing the acting forces and the magnitudes of these forces is shown in Figure 4.3. From this graph, it can be seen that the highest force acting is the magnetic force generated by the Earth's magnetic dipole. The smallest external force is gravity gradient. The period of one revolution of the satellite around the Earth is 98.03 min [24]. In Figure 4.4, the results of satellite's angular rotation rates are presented. This graph shows how fast the satellite with the modified attitude control system can settle when the attitude is changed. As it can be seen from the graph, the period is ~220 min until the satellite reaches stable orientation. The rotation rates vary from ±10 deg/sec (when satellite starts the movement) and stabilizes with ~ ±0.1 deg/sec rotation rates. It is worth to mention that this graph presents rotation rates during the launch of the satellite from the launching platform. The acting forces and moments represent boundary conditions and have the highest values. Hence, the values of rotation rates are substantial, and the strongest magnetic forces are needed for the stabilization. The proposed magnetic drive is sufficient for such tasks.

Numerical calculations of the satellite orbiting with an inclination of 98° in orbit were performed. This causes the angle between the satellite's nadir vector directed from the satellite to the Earth's center and the spherical rotor's magnetic field vector to change according to the sinusoidal law shown in Figure 4.5 (blue line). The change of the angle between the magnetic field vector of the spherical rotor and the Earth's magnetic field vector during the flight in the orbit is shown in red. It can be seen from the graph that the orientation of the nanosatellite with

respect to the Earth's magnetic field takes ~90 min. A change in the angle of the nadir vector indicates that the satellite completes the orbit around the Earth in approximately 95 min.

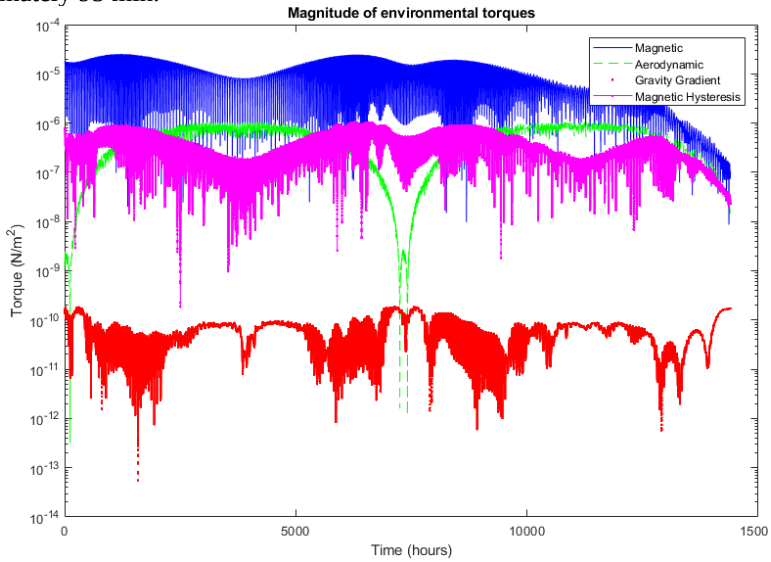

Figure 4.3. Summary graph of the acting external forces and their magnitudes

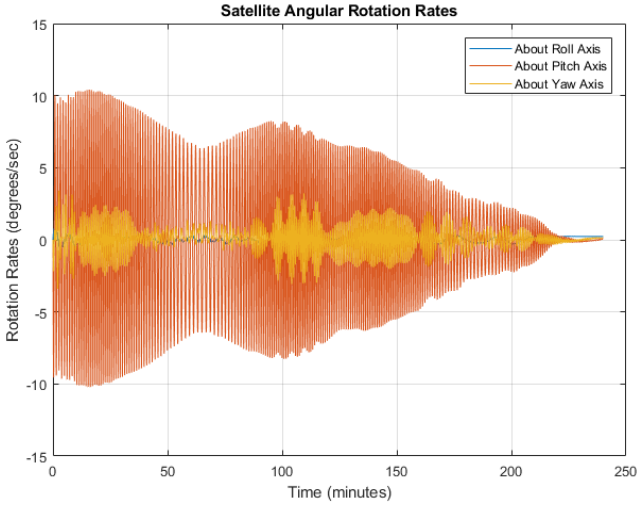

Figure 4.4. Satellite's angular rotation rates during the mission

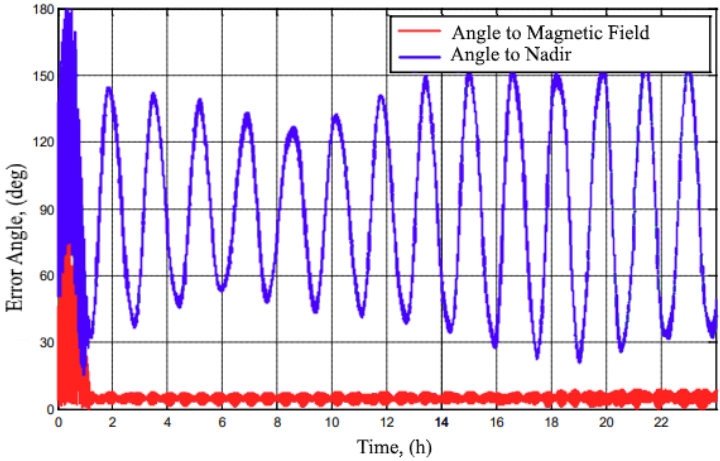

Figure 4.5. The change of satellite angles between nadir vector and satellite spherical rotor magnetic field vector during the satellite's mission

CONCLUSIONS

1. The development of suitable actuators used for the attitude control systems of the small satellites is analyzed. A comprehensive review of the existing multi-DOF piezoelectric ultrasonic drives revealed that compared to the electric motors of power consumption up to several dozen W, piezoelectric drives have great potential to be used in small satellites due to their small size, relatively high developing forces, and ability to operate in a vacuum. However, piezoelectric actuators as well have some disadvantages that make them difficult to use more widely: piezoelectric actuators usually generate displacements in only one axis, and if multi-axis movements are required, the systems become more complicated, more difficult to make such drive using automatization.
2. The simplified universal parametric FEA models of piezoelectric actuator have been created, which have been developed based on the proposed design of the ultrasonic piezoelectric motor. These models are used in numerical studies. Universal FEA models can be applied to the design of magnetospheric piezoelectric drives used for the attitude control systems of different configurations, adapting to CubeSat satellites with different characteristics and orbital altitudes up to 700 km.
3. Numerical and experimental studies of the developed piezoelectric actuators were performed, during which the vibration parameters of

actuators of several modifications and their influence on the actuator's dynamics were analyzed, and it has been determined that:

I. The operating frequencies of the investigated actuators vary in the ultrasonic range from 90 to 100 kHz. It has been observed that the electrical impedance at the resonant frequency, when the control electrode is divided into a different number of segments, varies insignificantly, but a capacitance of different electrode segmentation configurations differs almost threefold, when comparing configurations with 3 segments and 9 segments. And this directly affects the energy efficiency of the drive;

II. Actuators have several resonant zones, but practically significant of them are at ~ 60 kHz and ~ 92 kHz. Accordingly, in the first of them, the displacements are higher, but these displacements dominate in the radial and tangential axes, which is unfavorable for the formation of the rotational motion of the rotor, as it is difficult to ensure motion stability and controllability. When the piezoelectric element is excited in the ~ 92 kHz, the dominant displacements of contact point are generated in the radial and axial directions, but although the amplitude decreases by about 1–2 times compared with ~60 kHz, the drive control improves, and the sphere rotation becomes smoother. The sphere is rotated in a directional manner;

III. The actuator configuration with a disk-shaped flange is more effective, because the amplitude of oscillations generated by this actuator is 15% larger than the actuator with a triangle shaped flange;

IV. The average angular displacement resolution is ~ 30 μrad ±1 μrad, when the actuator is excited with burst-type electric signal of 60 V and frequency of 92 kHz. Such a resolution is sufficient to ensure the positioning accuracy of the spherical magnetic dipole vector with respect to the Earth's magnetic field;

V. The maximum angular velocity of the spherical rotor at the steady-state operation mode of the drive with a disk-shaped flange is ~ 30 rpm ±2 rpm and with a triangular flange ~ 27 rpm ±2 rpm;

VI. The analysis of the results of numerical simulations and experiments show some differences: in the case of ring-shaped piezoelectric transducer studies, it reaches ~ 1%, the actuators with flanges of different shapes ~ 2–3%. The probable reasons for these discrepancies are the inaccuracy of the material

properties used in the numerical simulations and prototype fabrication, FEA models created under idealized conditions, the influence of the glue layer and wire soldering, etc.

4. The satellite ESTCube-1 design modifications were executed: the existing attitude control mechanism was replaced by a MPD, and numerical studies were performed. A modified 1U satellite model was used for the mission analysis, and it has been found:
    I. The proposed MPD model occupies ~ 10% less volume and weight than the standard drive that was installed on this satellite during the imitational mission and ensures 3D active attitude control in space;
    II. The forces generated by a spherical permanent magnet used in the MPD are generating sufficient driving force to orient the satellite in a determined circular orbit of up to 700 km. The satellite, flying in the orbit and actively controlled by MPD, can change its angular orientation and reaches a stationary position within ~ 200 minutes from the start of the mission/change of position.

LIST OF REFERENCES

[1] B. Kang and J. Won, "Micro-Navigation Satellite Network Design and Analysis," in *Proceedings of 21st Internation Technical Meeting of the Satellite Division of the Institute of Navigation*, Savanah, GA, 2008.

[2] J. Uchino and J. R. Giniewicz, Micromechatronics, New York: Marcel Dekker Inc., 2003, pp. 1-32.

[3] F. Mends, "What Are Piezoelectric Materials?," 09 09 2019. [Online]. Available: https://sciencing.com/piezoelectric-materials-8251088.html. [Accessed 29 06 2020].

[4] K. Ragulskis, Vibrotechnika 50, Kaunas: VĮ Mokslotyros institutas, 2013.

[5] M. Chen-Glasser, L. Panpan, J. Ryu and S. Hong, "Piezoelectric Materials for Medical Applications," in *Piezoelectricity. Organic and Inorganic Materials and Applications*, 2018.

[6] I. Grybas, "Research and development of a high-resolution piezoelectric rotary stage: Doctoral dissertation," KTU, Kaunas, 2017.

[7] M. Hustig, "Piezoelectric Inertia Motors - A Critical Review of history, Concepts, Design, Applications and Perspectives," *Actutuators*, vol. 6, no. 7, p. 35, 2017.

[8] R. Vaccanore and R. Möller, "https://www.piceramic.com/," in *Cryogenic Behavior of Piezoelectric Bimorph Actuators*, 2000, pp. 275-282.

[9] B. Hu, .. Tang, W. Yan, S. Hu and Z. Hu, "Research on micro-displacement driving technology based on piezoelectric ceramic," in *Proc. SPIE 8418, 6th International Symposium on Advanced Optical Manufacturing and Testing Technologies: Design, Manufacturing, and Testing of Smart Structures, Micro- and Nano-Optical Devices, and Systems*, Xiamen, China, 2012.

[10] E. Steltz, M. Seeman, S. Avadhanula and R. Fearing, "Power Electronics Design Choice for Piezoelectric Microrobots," in *EEE/RSJ International Conference on Intelligent Robots and Systems*, Beijing, 2006.

[11] NASA, "Basic Concepts and Processes for First-Time CubeSat Developers," NASA, 10 2017. [Online]. Available: https://www.nasa.gov/sites/default/files/atoms/files/nasa_csli_cubesat_101_508.pdf. [Accessed 22 06 2020].

[12] E. S. Agency, "CubeSat - Deployer standards," European Space Agency, [Online]. Available: https://earth.esa.int/web/eoportal/satellite-missions/c-missions/cubesat-deployer. [Accessed 22 06 2020].

[13] ISO, "ISO 17770:2017(en) Standard," 2017. [Online]. Available: https://www.iso.org/obp/ui/#iso:std:iso:17770:ed-1:v1:en. [Accessed 22 06 2020].

[14] M. Ovchinnikov, "Methods to Control the Attitude Motion of a Satellite by EARTH's Magnetic Field," *Cooperation in Space, Euro-Asian Space Week : where East and West finally meet, Singapore*, vol. 430, pp. 475-483, 23-27 11 1998.

[15] G. Nader, E. N. Silva and J. C. Adamowski, "Effective Damping Value of Piezoelectric Transducer Determined by Experimental Techniques and Numerical Analysi," in *ABCM Symposium Series in Mechatronics*, 2004.

[16] N. Granick and J. E. Stern, "Material Damping of Aluminum by a Resonant-Dwell Technique," Nasa, Washington, 1965.

[17] S. Rawashdeh, "Smart Nanosatellite Attitude Propagator (SNAP)," 2019. [Online]. Available: https://se.mathworks.com/matlabcentral/fileexchange/68652-smart-nanosatellite-attitude-propagator-snap. [Accessed 15 07 2020].

[18] "About Matlab," Matlab, [Online]. Available: https://www.mathworks.com/products/matlab.html. [Accessed 15 07 2020].

[19] S. Rawashdeh, "Passive Attitude Stabilization for Small Satellites," 2010.

[20] H. Schumann, A. Berres, O. Maibaum and T. Liebezeit, "Simulation-Based Testing of Small Satellite Attitude Control Systems," in *6th IAA Symposium on Small Satellites for Earth Observatio*, 2007.

[21] H. L. Koenigsmann and G. Gurevich, "AttSim, Attitude Simulation with Control Software in the Loop," *Microcosm*, p. 13.

[22] A. Slavinskis, S. Latt and I. Sunter, "ESTCube-1 nanosatellite for electric solar wind sail in-orbit technology demonstration," in *Proceedings of the Estonian Academy of Sciences*, 2014.

[23] E. M. Relations, "N° 12–2013: ESA's Vega launcher scores new success with Proba-V," 7 5 2013. [Online]. Available: http://www.esa.int/Newsroom/Press_Releases/ESA_s_Vega_launcher_scores_new_success_with_Proba-V. [Accessed 15 07 2020].

[24] "ESTCube-1 (Estonian Student Satellite-1)," Sharing Earth Observation Reources, 2015. [Online]. Available: https://directory.eoportal.org/web/eoportal/satellite-missions/e/estcube-1#Bw@hK13cHerb. [Accessed 16 07 2020].

[25] EstCube, "EstCube," [Online]. Available: https://www.estcube.eu/en/home. [Accessed 16 07 2020].

[26] H. Ehrpais, J. kutt, I. Sunter, E. Kulu, A. Slavinskis and M. Noorma, "Nanosatellite spin-up using magnetic actuators: ESTCube-1 flight results," *Acta Astronautica,* vol. 128, pp. 210-216, 2016.

[27] S. e. al., "ESTCube-1 In-Orbit Experience and Lessons Learned," *Aerospace and Electronic Systems,* vol. 30, no. 8, pp. 12-22, 2015.

[28] "DK3WN SatBlog," 2013. [Online]. Available: https://www.satblog.info/category/estcube-1/page/24/. [Accessed 25 07 2020].

LIST OF PUBLICATIONS RELEVANT TO THE DISSERTATION IN PEER-REVIEWED SCIENTIFIC PUBLICATIONS

Indexed in the Web of Science with Impact Factor

International publishers

1. Jūrėnas, V.; Kazokaitis, G.; Mažeika, D. 3DOF ultrasonic motor with two piezoelectric rings // Sensors: Special issue: Development of piezoelectric sensors and actuators. Basel: MDPI AG. ISSN 1424-8220. eISSN 1424-8220. 2020, vol. 20, iss. 3, art. no. 834, p. 1-14. DOI: 10.3390/s20030834. [Science Citation Index Expanded (Web of Science); Scopus; EI Compendex Plus] [IF: 3,031; AIF: 3,797; IF/AIF: 0,798; Q1 (2018, InCites JCR SCIE)]
2. Jūrėnas, V.; Kazokaitis, G.; Mažeika, D. Design of Unimorph Type Multi-DOF Ultrasonic Motor// Applied Sciences (ISSN 2076-3417): Special Issue: Ultrasonic Transducers and Related Apparatus and Applications. Basel: MDPI AG. Appl. Sci. 2020, 10(16), 5605; https://doi.org/10.3390/app10165605 [IF:2.4; Q2 (2018, InCites JCR SCIE)]

Articles in conference proceedings

1. Kazokaitis, G.; Jūrėnas, V.; Eidukynas, D. A study on nano satellite orientation and attitude control systems for laser communication technologies // Mechanika 2017: proceedings of the 22nd international scientific conference, 19 May 2017, Kaunas University of Technology, Lithuania /

Kaunas University of Technology, Lithuanian Academy of Science, IFTOMM National Committee of Lithuania, Baltic Association of Mechanical Engineering. Kaunas: Kaunas University of Technology. ISSN 1822-2951. 2017, p. 177-182

2. Kazokaitis, G.; Jūrėnas, V.; Eidukynas, D. Research and analysis of spherical magnetic drive for attitude control on nano satellites // Vibroengineering procedia: [29th International conference on vibroengineering, Vilnius, Lithuania, December 1st 2017]. Kaunas: JVE International. ISSN 2345-0533. 2017, vol. 15, p. 50-55. DOI: 10.21595/vp.2017.19431. [Scopus; Academic Search Complete]
3. Kazokaitis, G.; Jurenas, V. Spherical magnetic drive for attitude control on nano satellites // Journal of applied mechanical engineering: conferenceseries.com joint event: 2nd international conference on advanced robotics, mechatronics and artificial intelligence and 3rd international conference on design and production engineering: December 03-04, 2018, Valencia, Spain. Hyderabad: OMICS International. ISSN 2168-9873. 2018, vol. 7, p. 73. DOI: 10.4172/2168-9873-C2-020.
4. Kazokaitis, G.; Jurėnas, V. Spherical piezoelectric magnetic drive // Mechanika 2019: proceedings of the 24th international scientific conference, 17 May 2019, Kaunas University of Technology, Lithuania / Kaunas University of Technology, Lithuanian Academy of Science, IFTOMM National Committee of Lithuania, Baltic Association of Mechanical Engineering. Kaunas: Kaunas University of Technology. ISSN 1822-2951. 2019, p. 76-79.

Presentation of the research results at conferences

Kazokaitis, G.; Jurenas, V. Spherical Piezoelectric Drive // 8th international conference on smart materials and structures, August 01–02, 2019, Dublin, Ireland. London: iMedPub. 2019, p. 34.

Patents

Gražvydas Kazokaitis; Vytautas Jūrėnas; Darius Eidukynas. Magneto pjezoelektrinės pavaros įrenginys; Patento Nr. LT 6728 B, 2020-04-10.

INFORMATION ABOUT THE AUTHOR

Gražvydas Kazokaitis was born in Pakruojis in 1988.
2006–2010: Studies in Kaunas University of Technology, Faculty of Mechanics and Mechatronics, Bachelor's degree in Mechanical Engineering.
2010–2012: Studies in Vilnius Gediminas Technical University, Faculty of Mechanics, Master's degree in Mechanical Engineering.
2016–2020: Doctoral studies in Kaunas University of Technology, Faculty of Mechanical Engineering and Design, (Technological Sciences, Mechanical Engineering (T 009)).
Email: grazvydas.kazokaitis@gmail.com

SANTRAUKA

Temos aktualumas

Šiuolaikinėse sistemose pjezoelektrinės pavaros bei įvairūs įrenginiai, pagaminti remiantis pjezoelektrinėmis medžiagomis ir jų savybėmis, yra plačiai paplitę ir naudojami įvairiose pramoninėse, mokslinėse bei plataus naudojimo prekėse. Įrenginiai, kurie turi pjezoelektrinę pavarą, gali būti sumontuoti: optinėse bei lazerinėse sistemose, mikromanipuliatoriuose bei mikrorobotuose, metrologiniuose įrenginiuose, medicinos prietaisuose, tikslaus medžiagų apdirbimo staklėse [1, 2]. Pjezoelektrinės pavaros yra preciziškos, kompaktiškos, nedidelės masės, tokių įrenginių maža inercija ir nedidelė atsako trukmė. Šios savybės leidžia pasiekti didelį galios ir masės santykį įrenginiuose, kur naudojami tokio tipo elementai.

Lietuvos mokslininkai vieni iš pirmųjų pasaulyje tyrė tokias problemas, sprendė įvairius precizinės vibromechanikos uždavinius, kūrė mechanizmus ir technologijas. Vibrotechnikos pradininkas Lietuvoje yra prof. habil. dr. K. Ragulskis, įkūręs vibrotechnikos laboratoriją ir mokyklą Kauno technologijos universitete (buv. KPI). Didelė dalis vibrotechnikos laboratorijos darbuotojų, žymiai prisidėjusių prie vibromechanikos uždavinių sprendimo, šios srities plėtojimo, tapo habilituotais mokslo daktarais, profesoriais: V. Augustaitis, R. Bansevičius, B. Bakšys, V. Barzdaitis, A. Bubulis, R. Barauskas, A. Busilas, J. Dulevičius, A. Fedaravičius, R. Jonušas, S. Kaušinis, A. Palevičius, G. Kulvietis, A. Kasparaitis, V. Ostaševičius, B. Spruogis, R. T. Toločka, V. Volkovas, P. Žiliukas ir daug kitų. Šių nusipelniusių mokslininkų dėka vibroinžinerijos mokslinėje srityje padaryti atradimai bei konstrukciniai sprendimai pritaikyti įvairiose srityse: mašinų bei prietaisų pramonėje, mokslo įrenginiuose, aerokosminėje technikoje, medicinoje, laivyboje ir kt. Šie mokslininkai suformulavo netiesinių dinaminių sistemų efektus bei principus, sukūrė mokslinius pagrindus ir principus naujų sistemų sudarymui, išplėtojo precizinės vibromechanikos sritį iki taikomųjų mokslų rezultatų panaudojimo

inžinerinei praktikai [3]. Nepaisant daugiamečio įdirbio vibromechanikos srityje tiek Lietuvoje, tiek ir pasaulyje, vis dar gausu neišspręstų bei atsirandančių naujų mokslinių uždavinių, susijusių su vibromechanika. Viena iš daugelio tokių sričių yra kosmoso pramonė ir joje kylančių iššūkių sprendimas bei naujų technologijų diegimas, kuris gali būti pagrįstas vibromechanikos principais.

Pjezoelektrinės pavaros yra gaminamos iš neferomagnetinių medžiagų ir gali būti naudojamos ten, kur neturėtų būti magnetinio lauko ar interferencijos su juo [4]. Šio tipo pavaros yra tylios, tad jas galima naudoti ten, kur aplinkos triukšmas yra nepageidaujamas, pvz., medicinoje, vaistų tiekimo sistemose ar išmaniuosiuose asmeniniuose įrenginiuose [3, 5]. Pjezoelektrinio tipo pavaras valdyti gana nesudėtinga – sužadinus tam tikru elektriniu valdymo signalu, pavarai yra suteikiamas tiesinis arba kampinis poslinkis. Pjezoelektrinės pavaros sunaudoja labai nedidelius energijos kiekius veikdamos statiniu režimu ir yra itin efektyvios, kai pavaros energetinės sąnaudos neviršija keleto dešimčių vatų lyginant su standartinėmis elektromagnetinėmis pavaromis. Pjezoelektrinėms pavaroms nereikalingas tepimas, tad tokios pavaros tinka naudoti ten, kur tepimas yra nepageidaujamas: pavaras sunku ar neįmanoma sutepti, siekiama išvengti tepalo garavimo aplinkoje, pvz., vakuume [6, 7]. Taip pat pjezoelektrinės pavaros esant darbiniam režimui kaista nežymiai, tad ši savybė leidžia naudoti tokio tipo pavaras ten, kur šilumos generavimas yra nepriimtinas. Pjezoelektrinės pavaros gali veikti itin žemose temperatūrose, siekiančiose keletą kelvinų [8].

Kadangi pačios pavaros yra nesudėtingos, o jų valdymo moduliai paprasti, tokių pavarų kaina santykinai nedidelė. Pjezoelektrinės pavaros lengvai pritaikomos prie reikalingų uždavinių bei integracijos reikalavimų.

Ultragarsinės stovinčiosios ar bėgančiosios bangos pavaros yra išsamiai nagrinėtos kaip galimas analogas tipinėms elektromechaninėms pavaroms, tačiau, nepaisant anksčiau paminėtų privalumų, šio tipo pavaros turi ir tam tikrų trūkumų, kurie apriboja galimą tokių pavarų panaudojamumą: pavarų poslinkių dydis ir pavarų matmenys negali būti didinami, kartais nepakankamas pavarų tikslumas, kontaktinių paviršių dėvėjimasis, pavarų kūrimo gamybos išlaidos tampa ekonomiškai nenaudingos. Tad vis dar atliekama nemažai tyrimų ir bandymų, kaip tokio tipo pavaras modifikuoti, norint išvengti anksčiau minėtų trūkumų bei susijusių problemų ar juos sumažinti.

Siekiant panaudoti pjezoelektrines pavaras palydovams reikia pažymėti, kad šio tipo pavaros užima nors ir nedidelį, bet tam tikrą tūrį, joms reikalingas valdymo modulis bei energijos šaltinis, kuris užtikrintų stabilų pavaros darbą, taip pat reikalingi matavimo ir grįžtamojo ryšio elementai, kuriuos pasitelkus galima sekti pavaros poziciją jos veikimo metu. Visi šie elementai turi būti integruojami į palydovą, jo valdymo bei sekimo sistemą.

Nepaisant keliamų reikalavimų bei tam tikrų trūkumų, kuriuos turi pjezoelektrinės pavaros ir kurie yra paminėti anksčiau, jos gali būti panaudojamos mažiems palydovams: šių pavarų masė ir dydis yra tinkamas, jų energijos

sąnaudos pakankamai mažos, užtikrina didelį išėjimo grandies generuojamo poslinkio tikslumą, joms nereikia tepimo, tad gali dirbti vakuumo aplinkoje ir žemose temperatūrose.

Tyrimo tikslas ir uždaviniai

Šio tyrimo tikslas – sukurti ir ištirti kelių laisvės laipsnių magnetosferinę pjezoelektrinę sukimo pavarą, skirtą aktyviai nanopalydovų orientacijai erdvėje.

Tikslui pasiekti iškelti tokie uždaviniai.

1. Atlikti egzistuojančių pjezoelektrinių pavarų konstrukcijų analizę, siekiant nustatyti jų panaudojimo galimybes aktyviai bei pasyviai nanopalydovų orientacijai erdvėje, pagerinti palydovo pozicionavimo tikslumo ir energinio naudingumo charakteristikas.
2. Suprojektuoti pjezoelektrinės pavaros, skirtos aktyviai trimatei nanopalydovų orientacijai erdvėje, skaitinius modelius, atlikti jos valdymo režimų patikrą ir ištirti dinamines charakteristikas bei keitiklio valdymo elektrodų konfigūracijos įtaką daugiakrypčių virpesių žadinimui.
3. Sukurti pjezoelektrinės pavaros su sferiniu rotoriumi eksperimentinį maketą atsižvelgiant į analitinius skaičiavimus ir atlikti valdymo režimų bei dinaminių parametrų eksperimentinius tyrimus su šiuo maketu.
4. Atlikti skriejančio nustatyta trajektorija aplink Žemę nanopalydovo simuliaciją, jo trimačiam orientavimui erdvėje naudojant sukurtą pjezoelektrinę pavarą su magnetiniu sferos formos rotoriumi, ir pateikti išvadas.

Tyrimo metodai

Šis darbas yra parengtas pasitelkiant teorinius bei eksperimentinius tyrimo metodus. Trimačių modelių sukūrimui bei jų analizei naudoti šie programiniai paketai ir įranga: *Autodesk Inventor Professional 2018*, *COMSOL MultiPhysics 5.3*, *Microsoft Excel* bei *Matlab 2017a* su papildiniais *Simulink* ir *Smart Nanosatellite Attitude Propagator (SNAP) V3.0*.

Eksperimentiniai tyrimai atlikti Kauno technologijos universiteto, Mechatronikos instituto laboratorijose. Pjezoelektrinės pavaros virpesių dinaminių parametrų tyrimams bei poslinkių matavimams atlikti naudoti lazeriniai Doplerio vibrometrai *Polytec PSV-500-3D-HV* ir *OFV-5000/505* bei signalų generatorius *WW5064* (*Tabor Electronics Ltd.*) ir įtampos stiprintuvas *EPA-104* (PiezoSystems Inc.). Impedanso tyrimams atlikti naudotas *Wayne Kerr 6500B* impedanso analizatorius. Sferos magnetinio lauko stipriui matuoti naudotas trijų ašių magnetometras, modelis 460 (*Lake Shore Cryotronics, Inc.*).

Mokslinis naujumas

1. Sukurta nauja pjezoelektrinė ultragarsinė sukamojo judesio trimatėje erdvėje pavara, pasižyminti dideliu sferinio rotoriaus pozicionavimo tikslumu ir leidžianti atlikti palydovo trimačio orientavimo erdvėje funkcijas.
2. Sukurtas ir ištirtas aukštesnių virpesių modų pagrindu funkcionuojantis pjezoelektrinis ultragarsinis vykdiklis, kurio aukštesnės modos virpesių žadinimui nustatyti ir apskaičiuoti keitiklio geometriniai parametrai bei efektyviam valdymui reikalinga valdymo elektrodų konfigūracija.
3. Sudaryti ir ištirti unimorfinio tipo žiediniai pjezoelektrinio keitiklio skaitiniai modeliai judesio trajektorijų tyrimui.

Ginamieji teiginiai

1. Sukurta ultragarsinė pjezoelektrinė pavara su sferiniu rotoriumi, kuri pasižymi dideliu kampinio poslinkio tikslumu (skyra 30 µrad ± 1 µrad), ir kuri gali būti panaudota mažų palydovų aktyvaus orientavimo trimatėje erdvėje sistemose.
2. Sukurtas bei ištirtas ultragarsinės pavaros pjezoelektrinis vykdiklis, kurio darbinis rezonansinis dažnis yra ~95 kHz, nustatyti bei apskaičiuoti vykdiklio geometriniai parametrai ir dinaminės charakteristikos, kurie yra reikalingi siekiant surasti efektyviausią jo valdymo elektrodų sudalinimo konfigūraciją.
3. Sudaryti unimorfinio tipo pjezoelektrinių žiedo formos vykdiklių skaitiniai modeliai, kurie skirti nagrinėti jo atskirų taškų erdvinių virpesių amplitudėms ir judesio trajektorijoms bei rezonansiniams darbiniams dažniams.

Praktinė vertė

1. Sukurti trimačiai pjezoelektrinės pavaros modeliai, kuriuos naudojant galima atlikti skaičiavimus, nagrinėti įvairias pavaros konfigūracijas, vykdyti teorinius tyrimus.
2. Daugiakanalis elektrinio valdymo signalo modulis gali būti naudojamas pjezoelektrinių ultragarsinių pavarų tyrimui su skirtinga valdymo elektrodų konfigūracija ir/ar kitokios geometrijos pjezoelektriniams keitikliams.
3. Sukurtas ir ištirtas unimorfinio tipo žiedinis pjezoelektrinis vykdiklis su keliomis jungės formomis, veikdamas aukštesnės modos virpesių režimu užtikrina didesnį sferinio rotoriaus kampinio poslinkio tikslumą ir yra energetiškai efektyvesnis.
4. Sukurta pjezoelektrinės pavaros konstrukcija gali būti naudojama ne tik aktyviam palydovų orientavimui, bet ir robotikoje,

optomechanikos inžinerijoje bei kitose tikslaus pozicionavimo sistemose.

Pirmas skyrius: literatūros apžvalga. Šiame skyriuje apžvelgiami pozicionavimo ir orientavimo mechanizmai, valdymo metodai, kurie šiuo metu yra naudojami palydovams. Vėliau aprašomos pjezoelektrinės medžiagos, pjezoelektrinių pavarų tipai. Skyrius užbaigiamas egzistuojančių pjezoelektrinių pavarų konstrukcine analize, pažymint šių pavarų trūkumus bei privalumus, konkretizuojamos savybės, kurias galima taikyti projektuojant pjezoelektrinės pavaros su sferiniu rotoriumi, skirtos nanopalydovų orientavimo ir pozicionavimo mechanizmui, eksperimentinį maketą.

Antras skyrius: čia pristatoma magnetosferinės pjezoelektrinės pavaros (MPP) konstrukcija, veikimo principas. Vėliau aprašomas baigtinių elementų metodui pritaikytas MPP modelis, pateikiama skaitinių tyrimų seka bei skaičiavimo metodai. Galiausiai aptariami atlikti MPP skaitiniai tyrimai, gauti rezultatai bei pateikiamos skyriaus išvados.

Trečias skyrius: jo pradžioje aprašomas eksperimentinis natūrinis MPP maketas. Tolimesniuose poskyriuose aprašomi atlikti pavaros natūriniai eksperimentai – impedanso skaičiavimai, rezonansinių dažnių bei virpesių formų tyrimai, kampinio poslinkio skyros nustatymas, vieno aktyvaus taško poslinkio tyrimas bei pavaros sukimosi dažnis. Skyriaus pabaigoje pateikiamos apibendrinamosios trečiojo skyriaus tyrimų išvados ir gauti rezultatai.

Ketvirtas skyrius: šio skyriaus pradžioje aprašomi palydovų misijos planavimo ir įgyvendinimo etapai. Tolesniuose poskyriuose pristatoma *ESTCube-1* palydovui pritaikyta MPP, galima jos integracija į palydovo konstrukciją. Vėliau skyriuje apibrėžiami kriterijai, kurie reikalingi siekiant atlikti palydovo skaitinę misijos analizę. Suskaičiuojami palydovo su MPP misijos skaitinei analizei reikalingi parametrai, atliekama skaitinė analizė bei pateikiami gauti rezultatai. Skyriaus pabaigoje pateikiamas palydovų pozicijos kontrolės sistemos aprašas, reikalingi jutikliai grįžtamajam ryšiui iš MPP gauti ir analizuojamas palydovo kontrolės sistemos veikimo algoritmas. Skyrius pabaigoje pateikiamos išvados.

Išvados: apibendrinami ir pateikiami atliktų teorinių bei eksperimentinių tyrimų rezultatai.

Priedai: pateikiamas išsamus misijos planavimo žingsnių ir vykdymo aprašas, pozicionavimo ir orientavimo sistemų bandymų įrangos veikimo principai bei eksperimentiniai metodai. Prieduose taip pat pateiktas SNAP, naudojamos palydovų misijos skaitinėms analizėms, programinės įrangos algoritmas.

Išvados

1. Išryškinti pagrindiniai įvairių pavarų, kurios naudojamos palydovams pozicionuoti ir orientuoti erdvėje, tipų privalumai ir trūkumai. Pavarų projektavimui aktualūs, misijoje veikiantys momentai, yra 8×10^{-8} Nm–1×10^{-8} Nm rėžyje. Rotorinių pavarų tipų analizė atskleidė, kad lyginant su elektros varikliais iki keliasdešimties vatų galios, pjezoelektrinės pavaros dėl savo mažo dydžio, sąlyginai didelių pasiekiamų jėgų ir galimybių dirbti vakuumo sąlygomis turi didelį potencialą būti panaudotos mažuosiuose palydovuose. Tačiau pjezoelektrinės pavaros turi ir trūkumų: jos dažniausiai generuoja poslinkius tik viena ašimi, jei reikalingi daugiaašiai poslinkiai, sistemos tampa sudėtingesnės. Taip pat tokios pavaros negali būti panaudotos ten, kur reikalingos didesnės pasiekiamos jėgos – pjezoelektrinės pavaros nepasiekia pakankamo našumo. Kompaktiškų pjezoelektrinių pavarų gamyba sunkiau automatizuojama, o palydovuose kompaktiškumas yra vienas iš reikšminių kriterijų.
2. Realizuoti supaprastinti universalūs parametriniai pjezoelektrinės pavaros BE modeliai, kurie buvo sudaryti remiantis suprojektuota pavaros konstrukcija: kai pjezoelektrinis keitiklis turi skirtingą žadinimo elektrodų skaičių ir yra su skirtingos geometrijos jungėmis, tokiu būdu suformuodamas unimorfinį vykdiklį. Universalūs BE modeliai gali būti pritaikomi projektuojant skirtingų konfigūracijų magnetosferines pjezopavaras, adaptuojant skirtingų charakteristikų bei orbitos aukščių *CubeSat* tipo palydovams.
3. Atlikti sukurtos pjezoelektrinės pavaros, vykdiklių dinaminiai skaitiniai ir eksperimentiniai tyrimai, kurių metu buvo nagrinėjamos kelių modifikacijų vykdiklių virpesių charakteristikos bei jų įtaka pavaros dinamikai, ir nustatyta, kad:
    I. Vykdiklių rezonansiniai (darbiniai) dažniai kinta 90–100 kHz rėžyje. Pastebėta, kad elektrinis impedansas rezonansiniame dažnyje, kai valdymo elektrodas sudalintas į skirtingą segmentų skaičių, kinta nežymiai, skirtingų elektrodo sudalinimo konfigūracijų talpis skiriasi beveik tris kartus, kai lyginamas trijų segmentų (sudalinimas kas 120°) ir devynių segmentų (sudalinimas kas 40°) variantai. O tai tiesiogiai daro įtaką energetiniam pavaros efektyvumui, t. y. mažesnį elektrinį talpį turinčio pjezoelektrinio vykdiklio energetinės sąnaudos mažėja.
    II. Rezonansiniu režimu veikiančios pavaros vykdikliai turi keletą rezonansinių zonų, tačiau praktiškai aktualiausios iš jų – ties ~60 kHz bei ~92 kHz. Atitinkamai, pirmojoje iš jų poslinkiai yra didesni, tačiau šie poslinkiai dominuoja radialine ir tangentine ašimis, o tai yra nepalanku rotoriaus sukamojo judesio formavimui, nes sudėtinga užtikrinti judesio stabilumą bei valdomumą erdvėje.

Kai pjezoelektrinis elementas yra žadinamas ties ~92 kHz zona, dominuojantys kontaktinio taško poslinkiai yra generuojami radialine bei ašine kryptimis, vis dėlto, nors ir sumažėja amplitudė apie 1–2 kartus, lyginant su pirmąja rezonansinio piko zona, tačiau pagerėja pavaros valdomumas ir sferos sukimasis tampa tolygesnis, sfera sukama kryptingai.

III. Pranašesnė yra vykdiklio su diskine junge konfigūracija, nes šio vykdiklio poslinkių amplitudė yra 15 % didesnė nei vykdiklio su trikampe junge.

IV. Vidutiniškai rotoriaus kampinio poslinkio skyra siekia ~30 µrad ±1 µrad, žadinant 60 V ir 92 kHz elektriniu signalu. Tokia skyra yra pakankama tam, kad būtų užtikrinamas sferos magnetinio dipolio vektoriaus pozicionavimo tikslumas Žemės magnetinio lauko atžvilgiu, kuris yra reikalingas palydovo erdvinio pozicionavimo ir orientavimo sistemoms.

V. Pavaros su diskine junge maksimalus sūkių dažnis yra ~30 aps/min, o su trikampe junge ~27 aps/min, šis dydis gali būti valdomas, keičiant elektrinio signalo įtampos amplitudę. Toks sūkių dažnis yra pakankamas tam, kad palydovo magnetinio dipolio vektorius būtų orientuojamas pagal nurodytas koordinates Žemės magnetinio lauko atžvilgiu.

VI. Skirtumai tarp skaitinių ir eksperimentinių rezonansinių dažnių reikšmių yra nedideli: žiedinio keitiklio atveju siekia ~1 %; vykdiklių su skirtingų formų jungėmis ~2–3 %. Tikėtinos šių neatitikimų priežastys: netapačios medžiagų fizikinių charakteristikų skaitiniame ir natūriniame modelyje reikšmės, idealizuotos sąlygos sukurtuose BE modeliuose, valdymo elektrodų sudalinimo bei laidų litavimo įtaka ir kt.

4. Atlikus palydovo *ESTCube-1* konstrukcijos modifikaciją, egzistuojantis orientavimo ir pozicionavimo pavaros konstrukcinis mazgas buvo pakeistas magnetosferine pjezoelektrine pavara bei atlikta skaitinė analizė. Modifikuotas palydovo 1U modelis buvo naudojamas misijos analizei atlikti ir nustatyta, kad:

   I. Pasiūlytas pavaros konstrukcijos tūris ir masė ~10 % mažesni nei standartinė pavara, kuri buvo sumontuota šiame palydove imituojamos misijos metu ir užtikrina aktyvų trimačio (3D) palydovo orientavimą erdvėje.

   II. Magnetosferinėje pjezoelektrinėje pavaroje esančio nuolatinio magneto kuriamos jėgos pakaktų palydovui orientuoti, jam skriejant apskritimine orbita ne didesniame nei 700 km aukštyje. Palydovas,

skriedamas orbita, pasiekia stacionarią padėtį per ~200 minnuo misijos pradžios / pozicijos pakeitimo.

Darbo rezultatų aprobavimas

Disertacijoje pateikiami tyrimai buvo publikuoti įvairiuose leidiniuose bei konferencijose: dviejose *Web of Science* duomenų bazėje referuojamuose žurnaluose su dideliu citavimo indeksu ir keturiose publikacijose konferencijų pranešimų medžiagoje.
Tyrimų rezultatai pateikti šešiose tarptautinėse konferencijose: (*Mechanika 2017, 2019* (Kaunas, Lietuva); *Vibroengineering 2017* (Vilnius, Lietuva); *Advance robotics, mechatronics and artificial intelligence* (Valensija, Ispanija, 2018); *Smart Materials and Structures*, 2019 (Dublinas, Airija); *Mechatronic Systems and Materials*, 2020 (Bialystokas, Lenkija).

UDK 62-83-52(043.3)

SL344. 2021-*-*, * leidyb. apsk. l. Tiražas 50 egz.
Išleido Kauno technologijos universitetas, K. Donelaičio g. 73, 44249 Kaunas
Spausdino leidyklos „Technologija“ spaustuvė, Studentų g. 54, 51424 Kaunas